


Minh DUC DAO ¹, Xuan Tuy TRAN², Dang Phuoc PHAM¹,
Quoc Anh NGO¹, Thi Thuy Tram LE³

Study on the ankle rehabilitation device

Received 19 July 2021, **Revised** 10 November 2021, **Accepted** 16 November 2021, **Published online** 31 December 2021

Keywords: ankle, rehabilitation, stroke, slide mode controller, linear actuator

This study developed an ankle rehabilitation device for post-stroke patients. First, the research models and dynamic equations of the device are addressed. Second, the Sliding Mode Controller for the ankle rehabilitation device is designed, and the device's response is simulated on the software MATLAB. Third, the ankle rehabilitation device is successfully manufactured from aluminum and uses linear actuators to emulate dorsiflexion and plantarflexion exercises for humans. The advantages of the device are a simple design, low cost, and mounts onto rehabilitative equipment. The device can operate fast through experiments, has a foot drive mechanism overshoot of 0°, and a maximum angle error of 1°. Moreover, the rehabilitation robot can operate consistently and is comfortable for stroke patients to use. Finally, we will fully develop the device and proceed to clinical implementation.

1. Introduction

Stroke, a condition caused by blockage of blood supply to a part of the brain, is a serious life-threatening medical condition occurring more rapidly worldwide. Not only affecting older adults, but strokes also affect younger populations [1, 2]. A stroke is a medical emergency, and urgent treatment is needed to prevent death or significant neural damage. More than a half of stroke survivors are left with some form of hemiplegia. These patients experience difficulty in performing many activities of daily living (ADLs) due to limited mobility and feeding problems

✉ Minh DUC DAO, e-mail: dmduc@pdu.edu.vn

¹Faculty Technology and Engineering, The Pham Van Dong University, Quang Ngai, Vietnam; ORCID (M.D.D.): 0000-0003-3086-1912

²Faculty Technology of Mechanical Engineering, The University of Danang – University of Science and Technology, Danang, Vietnam

³The Faculty Electronic-Electrical, The Quang Nam College, Quang Nam, Vietnam



© 2022. The Author(s). This is an open-access article distributed under the terms of the Creative Commons Attribution-NonCommercial-NoDerivatives License (CC BY-NC-ND 4.0, <https://creativecommons.org/licenses/by-nc-nd/4.0/>), which permits use, distribution, and reproduction in any medium, provided that the Article is properly cited, the use is non-commercial, and no modifications or adaptations are made.

[3, 4]. The essential joint during the rehabilitation of the lower limb is the ankle joint, a complex bone structure in the human body. Contracture with the ankle joint due to stroke can critically limit the mobility of stroke survivors [5, 6]. An early start to mobility training for stroke patients would improve patients' chances of recovering the lost ability [7, 8]. In this work, we will study a viable device that can accelerate such mobility training.

Special attention has been given to post-stroke rehabilitation for motor function recovery. These components of training include stretching exercises, gait training, constraint-induced movement therapy (CIMT), and other learning mechanisms aimed at stimulating neuroplasticity. However, the main problem with the current therapeutic practices is that a single physiotherapist administers it to an individual patient. This limitation results in less frequent Physical Therapy (PT) sessions and lengthening recovery time [9]. Robot assistance has been proposed as a resolution of these issues to support physicians in providing effective therapies. In particular, ankle rehabilitation robots can relieve physiotherapists of repetitive tasks and provide the opportunity to treat multiple patients simultaneously.

Furthermore, there are more benefits of this approach for patients. For example, mobility treatment through robots allows more comprehensive data collection, which leads to better monitoring of patients' recovery progress. Additionally, robot-assisted therapies can be easily organized into games that help to improve patients' mentality when therapies are administered [10, 11].

These robots can be roughly classified into two groups according to their mechanical Degree of Freedoms (DOF): the first group consists of rehabilitation robots with multiple DOFs, and the second one constitutes of robots with 1-DOF.

In the first group, Sun et al. [12] developed a novel ankle rehabilitation robot composed of a base platform and a rotating platform connected by three linear actuators and a connecting rod. The motor drives the rotating platform, and ankle movement is simulated. Liu et al. [13] developed the device which has 3-DOF with the design of a similar platform connected using pneumatic muscles. Yonezawa et al. [14] also develop an ankle-foot device employing a Stewart platform and six pneumatic cylinders that operate synchronously. The advantages of this device group consist in treating patients with all 3 degrees of freedom, so the human ankle joint is fully mobilized. Thus, the devices will help shortening the training time for the patient. The disadvantages are that the devices will have a more complex structure, so controlling their operation requires high accuracy and fast response. In addition, the controller requires multiple input parameters to control patient's movements accurately.

In the second group, Ye Ding et al. [15] introduced a device to support rehabilitation exercises for the ankle joint in plantar flexion/dorsiflexion. The authors used the Labview software to control and monitor the exercises. Ao et al. [16] presented a control method for an ankle rehabilitation exercise device using an EMG sensor to measure the impact moment of the muscle force. Ren et al. [17] presented a device to support rehabilitation exercises for ankle joints at the bed;

the device has additional game simulation software to help patients increase the excitement when participating in the exercise. Aguirre-Ollinger et al. [18] have designed and manufactured an exercise support device for ankle joints, in which the driving mechanism is an AC servo motor, and which has a built-in model of interaction between the patient and the equipment. The authors designed the transfer function for the model and used the LQ controller to control it. Zhuo et al. [19] also introduced a training device for the ankle joint with plantarflexion/dorsiflexion by combining the EMG force sensor and the torque sensor on the motor shaft. The authors used a PID controller and designed a screen monitor to control the device's parameters using the LabView software. The advantage of these devices is that they have a simple structure, focusing on controlling one joint, so the treatment support for the patient will have a higher efficiency. There are some disadvantages of these devices. The studies [16–19] have not yet provided the dynamic equations of the device and controller. The authors of [18] and [19] have introduced an application of a PID controller and an LQ controller; however, the kinematic equation of the device has not been presented clearly. The above devices use the driving mechanism consisting of a DC motor [16–18] and an AC motor [19]. Then, to ensure the device's safety, it is necessary to consider the situation when there occurs a sudden change of load. The above devices do not have such a high self-braking ability to protect the patient in the case of overload.

In this paper, we present a device that supports rehabilitation exercises for ankle joints in the plantarflexion/dorsiflexion movement, which has a simple structure and is easy to control. Furthermore, the device uses a reciprocating mechanism to drive, so it will create a high self-braking ability because the structure of the mechanism is a screw and nut drive. Hence, our work presented in this paper focuses on developing dynamic equations for the ankle drive mechanism and building a Sliding Mode Controller (SMC) for the actuator based on the dynamical model developed by the authors to precisely adjust the foot drive platform. Furthermore, we differentiate our research from the previous ones by focusing on a robust, simple, and low-cost design. The device is then designed and simulated on the Matlab before being manufactured and clinically tested to compare our results with similar studies. The paper is organized as follows. In section 2, we introduce the research model and the dynamic equation of the device. Section 3 presents the controller for the device and simulation results of the device's response using the Matlab software. The results of fabrication, testing of the device, and discussion are presented in section 4. Finally, the conclusions are given in section 5.

2. Theoretical basis of ankle rehabilitation device

2.1. Kinematic model of ankle rehabilitation device

The ankle joint has a structure of 3 degrees of freedom, and Fig. 1 shows the exercises for the ankle joint [20]. According to [20], the range of motion

of the human ankle joint in the plantarflexion/dorsiflexion has the most significant amplitude (0° – 80°), and the movement requires the most significant impact torque.

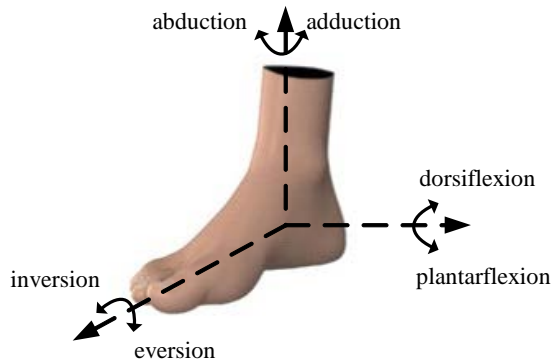


Fig. 1. The movements of the human ankle joint

In this study, we designed an ankle rehabilitation robot with the 1-DOF rotational motion to facilitate plantarflexion and dorsiflexion. The device converts the linear impact force from linear actuators into the torque around the shaft, so this torque rotates the foot platform to emulate dorsiflexion/plantarflexion rotations. The kinematic model of the ankle rehabilitation device is presented in Fig. 2, with the foot drive mechanism rotating the patient foot platform up to 80° . The rotational angle θ depends on the ankle flexion exercise, dorsiflexion at angles $0^{\circ} \leq \theta \leq 30^{\circ}$, and plantarflexion at $-50^{\circ} \leq \theta \leq 0^{\circ}$. To control the motion angle of the ankle joint, we will control the position of the linear actuator so that the rotation angle θ will be proportional to the position of the linear actuator.

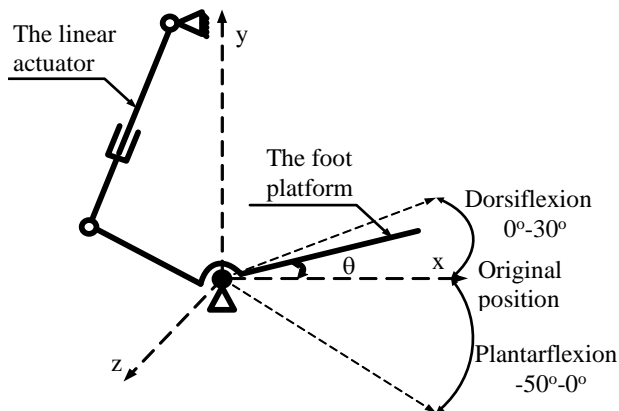


Fig. 2. The schematic diagram of the ankle rehabilitation device

2.2. Dynamic equations of the ankle rehabilitation device

Establishing the dynamic equations for each device component is an essential aspect of determining how the device interacts with patients' joints, which helps one to improve the mechanical design and tuning the controller system to best match patients' needs. Generally, we followed the approach described in previous studies [21–23] to establish the dynamic equations for the device, and the foot drive mechanism which administered plantarflexion /dorsiflexion was assumed to be in a linear motion. In this paper, we establish the dynamic equation of the device based on the Lagrange method. To simplify the process of setting up the dynamic equation of the device, we assume that the mass of the human foot and the weight of the foot platform can be reduced to a total mass M . The torque required to lead the movement of the human ankle joint is τ , which is the moment created by the linear actuator. Fig. 3 presents a dynamic diagram of the device. The linear actuator will create a force F , acting on the joint with the foot platform. Therefore, the necessary torque will be generated to drive the foot platform to rotate around the axis, thereby making the human ankle joint (in this case, the person's foot is fixed with the foot platform).

The kinetic energy of the foot drive mechanism:

$$K = \frac{1}{2}MR_C^2\dot{\theta}^2. \quad (1)$$

The potential energy of the foot drive mechanism:

$$P = MgR_C \sin \theta. \quad (2)$$

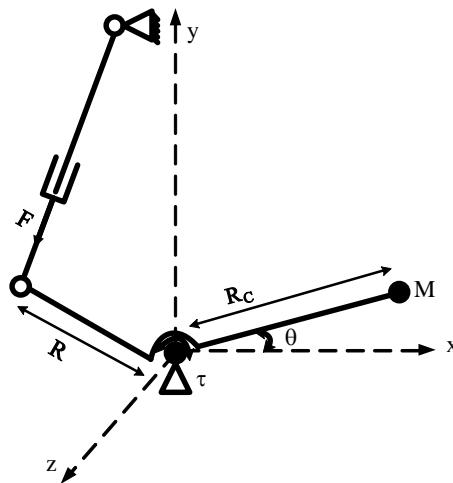


Fig. 3. The dynamic diagram of the ankle rehabilitation device

From Eq. (1) and Eq. (2), the Lagrange function for the foot drive mechanism:

$$L = K - P = \frac{1}{2}MR_C^2\dot{\theta}^2 - MgR_C \sin \theta. \quad (3)$$

The dynamic equation of the drive mechanism based on Euler-Lagrange equations:

$$\frac{d}{dt} \frac{\partial L}{\partial \dot{\theta}} - \frac{\partial L}{\partial \theta} = \tau. \quad (4)$$

During the operation of the device, factors such as the weight of the components and the force due to the patients will influence the device operation. From Eq. (3) substituted into Eq. (4), the dynamic equation for the force of the drive is derived according to [23]:

$$J\ddot{\theta} + D\dot{\theta} + G + \tau_D = \tau, \quad (5)$$

where: $J = MR_C^2$; $G = MgR_C \cos \theta$. D is drag coefficient of friction of the platform, τ_D is disturbance torque (torque created by the action of the human foot), M is mass of the human foot and the foot platform, and R_C denotes length of the foot platform.

Therefore, the angular acceleration can be obtained straightforwardly from the dynamic Eq. (5). Next, the equation is rewritten as:

$$\ddot{\theta} = J^{-1}(\tau - D\dot{\theta} - G - \tau_D). \quad (6)$$

3. Designing the controller and simulation

3.1. Design the sliding mode controller

In this study, we utilized the widely-used Slide Mode Controller (SMC) to control the device. SMC is often used in the speed control of electric drive systems. SMC is a nonlinear control method that alters the dynamics of a nonlinear system by applying a set-valued signal. The controller's response causes the linear actuator system to "slide" along a sliding surface. This controller has the advantages such as fast dynamic response, insensitivity to external disturbance, and readily available integration into the current system hardware. However, the controller undergoes small high-frequency switching during operation, and we overcome this effect using the sign or sat function for the controller [24]. The SMC controls the linear actuator using angle sensors of foot drive angle, and the sensors of angular velocity, acceleration, and the setpoint angle. The Slide Mode Controller is designed as follow:

The angular error is defined as:

$$e = \theta_d - \theta,$$

where θ_d is the setpoint angle.

The errors of angular velocity and angular acceleration are:

$$\begin{aligned} \dot{e} &= \dot{\theta}_d - \dot{\theta}, \\ \ddot{e} &= \ddot{\theta}_d - \ddot{\theta}. \end{aligned}$$

The motion of the state trajectory s on the sliding surface is defined as [25]:

$$s = \lambda e + \dot{e}, \quad (7)$$

where λ is a positive constant. Hence, the differential system equation is:

$$\dot{s} = \lambda \dot{e} + \ddot{e}. \quad (8)$$

The signal of the controller is the torque of the foot drive mechanism. This torque consists of two components [25]

$$u = \begin{cases} u_{eq} & \text{where } s = 0, \\ u_N & \text{where } s \neq 0. \end{cases} \quad (9)$$

The control signal for the SMC can be found by solving the equivalent control law on the sliding mode:

$$\begin{aligned} \dot{s} &= 0, \\ \dot{s} &= \lambda \dot{e} + \ddot{e} = 0, \\ \dot{s} &= \lambda \dot{e} + \ddot{\theta}_d - \ddot{\theta}, \\ \dot{s} &= \lambda \dot{e} + \ddot{\theta}_d - J^{-1}(\tau - D\ddot{\theta} - G - \tau_D), \\ &\Rightarrow \dot{s} = \lambda \dot{e} + \ddot{\theta}_d - J^{-1}(u_{eq} - D\dot{\theta} - G - \tau_D), \\ \dot{s} &= \lambda \dot{e} + \ddot{\theta}_d - J^{-1}(u_{eq} - D\dot{\theta} - G - \tau_D) = 0, \\ &\Rightarrow u_{eq} = J\lambda \dot{e} + J\ddot{\theta}_d + D\dot{\theta} + G + \tau_D. \end{aligned} \quad (10)$$

Assigning the direction signal for the actuator as the sign function u_N :

$$u_N = K \operatorname{sgn}(s), \quad (11)$$

where:

$$\operatorname{sgn}(s) = \begin{cases} 1 & s > 0, \\ -1 & s < 0, \\ 0 & s = 0. \end{cases}$$

Combining Eq. (11) and Eq. (10), one obtains the slide mode controller for the actuator illustrated by Eq. (12):

$$u = u_N + u_{eq} = K \operatorname{sgn}(s) + J\lambda \dot{e} + J\ddot{\theta}_d + D\dot{\theta} + G + \tau_D \quad (12)$$

where K is a positive constant.

To assess the stability of the SMC, the Lyapunov method was used. The Lyapunov function was defined as follows:

$$V(s) = \frac{1}{2}s^2.$$

Differential function:

$$\dot{V}(s) = \dot{s}s.$$

Deriving from equation (12):

$$\dot{V}(s) = -sK\text{sgn}(s).$$

For the SMC to be stable:

$$\dot{V}(s) = -sK\text{sgn}(s) < 0,$$

$$\dot{V}(s) = -K|s| < 0.$$

Then, if $K > 0$ (i.e., if K is positive definite), the system is asymptotically stable.

3.2. Simulation

After establishing the dynamics of the system and designing the control SLM for model research, we use the Matlab software to simulate the response of the model research. The control loop diagram of the model is shown in Fig. 4, the setting signal θ_d is the angle set of ankle joint actions, and the tracking response signal is θ . The SLM controller will rely on the error of rotation angle and the error of rotational velocity to generate the torque required for the device. In the control diagram, we added the torque τ_D in the dynamic effect of the external force (assuming the force impedance makes the muscle of the human foot work). The simulation parameters for the model research are shown in Table 1, where the coefficient D is referenced [26]. The constants λ and K of the SLM controller

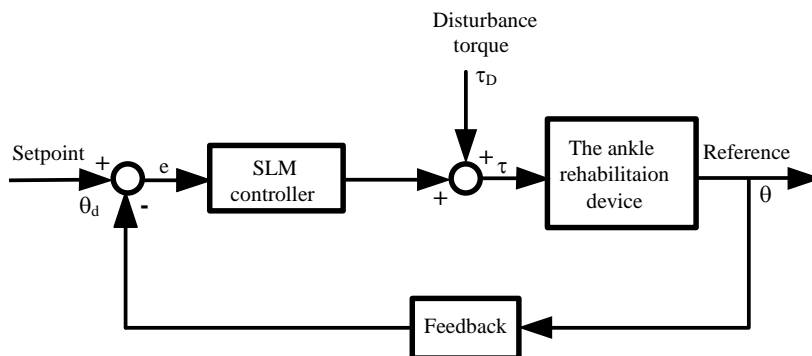


Fig. 4. The control diagram of the research model

Table 1. Simulation parameters for the research model

Mass of the human foot and the foot platform. (The maximum human's weight is 120 kg)	$M = M_{\text{foot}} + M_{\text{platform}}$ $= 120 \cdot 0.12 + 0.5 = 2 \text{ kg}$ [27]
Length of the foot platform	$R_C = 0.25 \text{ m}$
Constants	$K = 40; \lambda = 1$
Coefficient of friction of the platform	$D = 0.01 \text{ Nms/rad}$
Disturbance torque	$\tau_D = 5 \text{ Nm}$ [28]

employed for forcing the plant to behave like the model were set using a trial-and-error method. It is possible to fine-tune these controller gains, choose different gains for the controller, and reduce the amount of tracking error. The initial angle condition for the model simulation was $\theta(0) = 0^\circ$, the stimulation frequency was 0.25 Hz, and the set angle signal was sinusoidal. We simulated the ankle rehabilitation device operating with a slide mode controller during operation with the established dynamic equations. The simulation ran with the input setpoint angles for dorsiflexion and plantarflexion.

The simulation results are presented in Fig. 5. The simulation was performed with dorsiflexion action at angles $\theta_d = 15^\circ \sin(2\pi 0.25t) + 15^\circ$. The 30° angle of

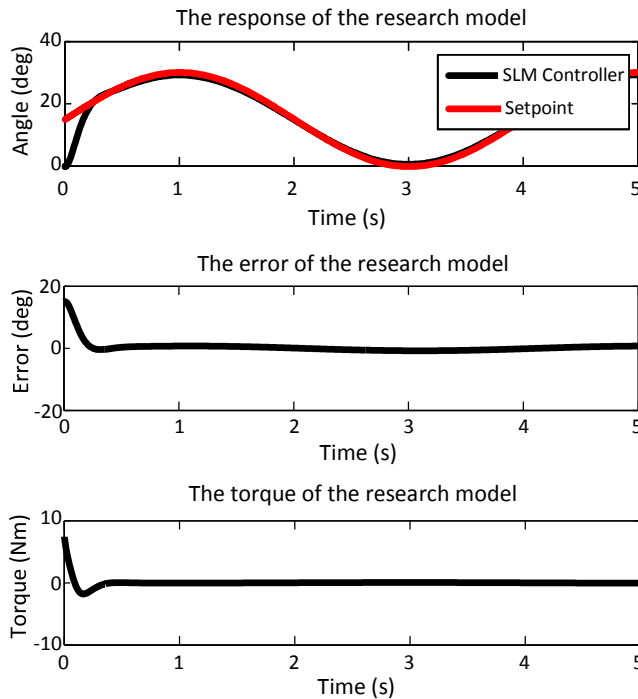


Fig. 5. Simulation results for dorsiflexion exercises. Graphs show setpoint angle (red) and reference angle (black) values for the ankle joint (top), angular error of the ankle joint (middle), the torque of angular error of the ankle joint (bottom)

dorsiflexion was chosen because it is the maximum plantarflexion angle of the ankle motion. Fig. 5 shows the input trajectory (red line) supplied to the device and the resulting output (black line). The simulation results show that the output trajectory follows the input trajectory closely with a small error (Fig. 5 shows the tracking errors in more detail). Furthermore, it can be seen that the maximum tracking error for the sequential joint was 0.5° . Therefore, the maximum torque produced for the dorsiflexion exercise was 7.5 Nm.

Another simulation was performed for the plantarflexion exercise with rotational angles $\theta_d = -\frac{50^\circ}{2} \sin(2\pi 0.25t) - \frac{50^\circ}{2}$, and the simulation results are presented in Fig. 6. The 50° angle of plantarflexion has been chosen because it is the maximum plantarflexion angle of the ankle motion. The results show that the device responds quickly to the setpoint angle, the overshoot is 0° , and the maximum tracking error is 0.4° . The maximum torque produced for the dorsiflexion exercise is 8 Nm. With the simulation results in the dorsiflexion/plantarflexion exercise of the research model, one obtains the maximum torque value of 8 Nm, which is consistent with the results in [29, 30]. The results are the basis for selecting parameters of the linear actuator and for application of the sliding mode control for programming of the device.

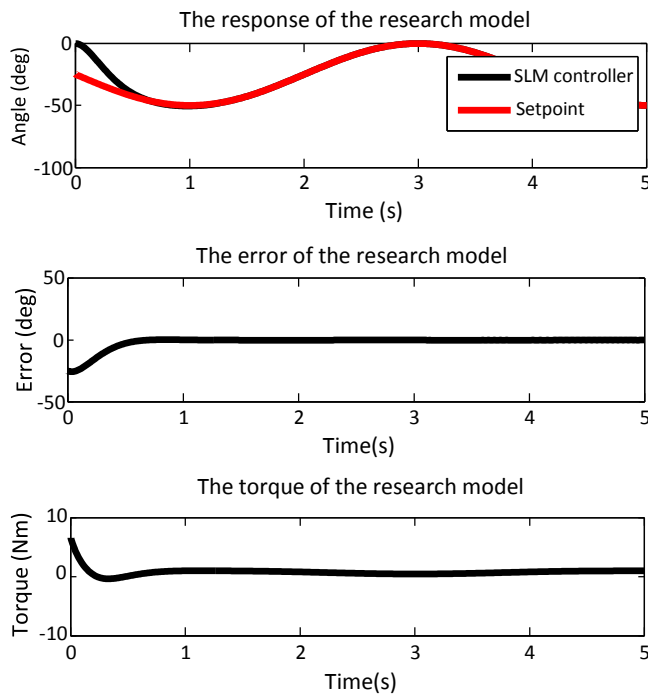


Fig. 6. Simulation results of plantarflexion exercise. Graphs show setpoint angle (red) and reference angle (black) values for the ankle joint (top), angular error of the ankle joint (middle), the torque of angular error of the ankle joint (bottom)

4. Manufacturing and testing

4.1. The ankle rehabilitation device

The device is manufactured from aluminum and stainless steel accurately with CNC and Lathe machines. An essential aspect of manufacturing is the cost and safety of the device. The device is robust and durable with aluminum shafts and the linear actuator encased in a hard plastic. The use of linear actuators reduces our cost, providing the ankle rehabilitation devices with a high potential for proper implementation. The fully functional prototype of the proposed ankle rehabilitation device is shown in Fig. 7. The device consists of the following four components: (i) The linear actuator that produces rotation of the foot platform by converting linear motion into rotation; (ii) The foot platform that supports and holds the person's foot in place with a strap, whose length is 25 cm; (iii) The shark platform which can be adjusted according to the person's size, and has a length of 40 cm; (iv) The encoder which is used to measure the angle of the human ankle joint during exercise.



Fig. 7. Prototype of the ankle rehabilitation device

Figs. 8 and 9 present the diagram and the flowchart of the ankle rehabilitation device. Firstly, the operator assigns rotational angles for the device through a computer. The computer then sends signals to the microprocessor onboard the device, using the programmed SMC controller to direct the linear actuator. The linear actuator rotates the ankle drive mechanism (i.e., the foot platform) and the patient's foot to the setpoint angle. In this device/prototype, we used the Arduino 2560 microprocessor to process the data from sensors and to control the linear actuators accordingly. We relied on Hall Effect sensors with 12-bit resolution. Moreover, the study employs an ACS712 sensor to monitor current values of the foot drive

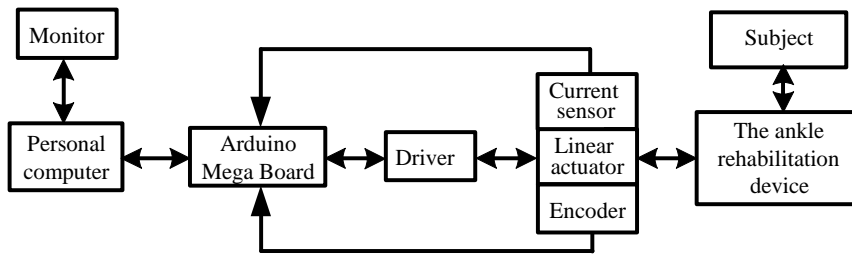


Fig. 8. Diagram of the ankle rehabilitation device

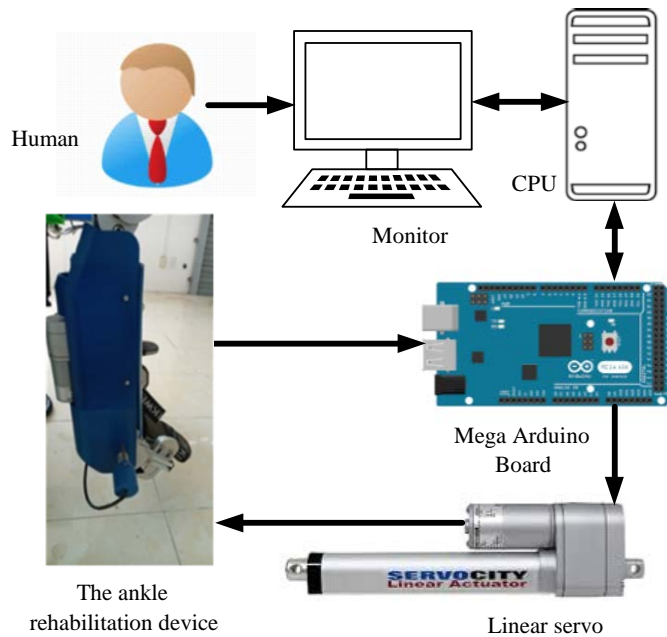


Fig. 9. Flowchart of the ankle rehabilitation device

mechanism to prevent electrocuting the users accidentally via the aluminum foot platform. Table 2 presents the parameters and prices of the components in the ankle rehabilitation exercise equipment.

Table 2. Parameters of the device

Name	Type	Main parameters	Cost
Linear actuator	HDLS-6-30-12V	Stroke length: 150 mm Voltage: DC 12 V; Max force: 500 N	300 \$
Encoder	Hall Sensor	Resolution: 12 bit	60\$
Sensor current	ACS712	Resolution: 10 bit	5 \$
Control board	Mega 2560	Voltage: DC 5 V	10 \$

4.2. Experiment results

The experiments in this study were performed on a male with a weight of 60 kg and a height of 170 cm (Fig. 10). The device emulated dorsiflexion and plantarflexion with the angles similar to the previous MATLAB simulations, because these were the ranges of motion of the human ankle joint. During these trials, safety features were incorporated, including an emergency stop button and the ACS712 current sensor on the ankle drive mechanism.



Fig. 10. Rotation cycle for the device with a human

The results of the trial for dorsiflexion exercise, illustrated in Fig. 11, show that the ankle rehabilitation device accurately rotates to each setpoint angle. The most significant recorded rotational error was 1° , and the most significant recorded current in the device was 1.5 A.

The results of the trial for the plantarflexion exercise, illustrated in Fig. 12, show that the ankle rehabilitation device accurately rotates to each setpoint angle. The most significant recorded rotational error was 1° , and the recorded current in the foot drive mechanism was 2.0 A. In this trial, due to a larger rotational angle required for the exercise, the torque due to the weight of the patient foot increased and resulted in a more significant current produced to compensate for the additional amount of torque.

Experimental results on humans with ankle flexion/extension show that the rotation angle error is small, proving that the sliding mode controller gives a good response to the simulation. Comparing these results with the study by Bucca et al. [31] we can see that the currents are similar. Comparison of the rotation angle error with the study of Zhong et al. [32] shows that our device gives better results (1° compared to 4.5°). In addition, the device has a more straightforward structure and its cost is lower [31, 32]; the total cost of the device is \$400.

The limitation of the study is that it has only been studied on healthy humans and has not been examined on stroke patients.

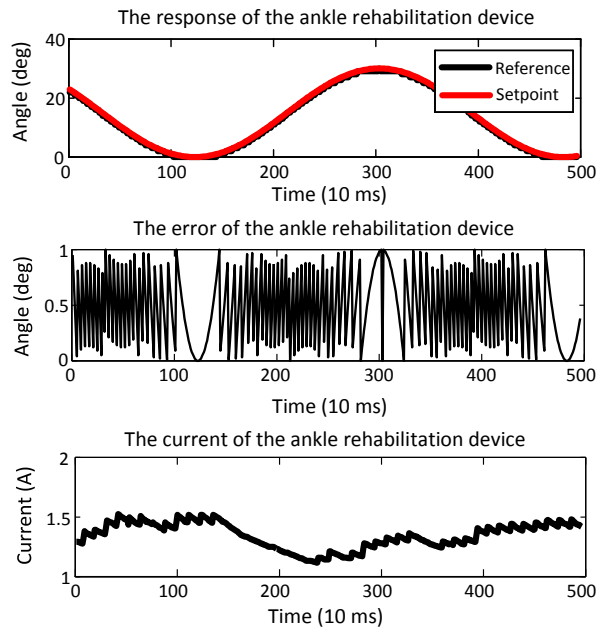


Fig. 11. Experiment results of dorsiflexion exercise with humans. Graphs show setpoint angle (red) and measured angle (black) values for the device (top), angular error of the device (middle), current of the device (bottom)

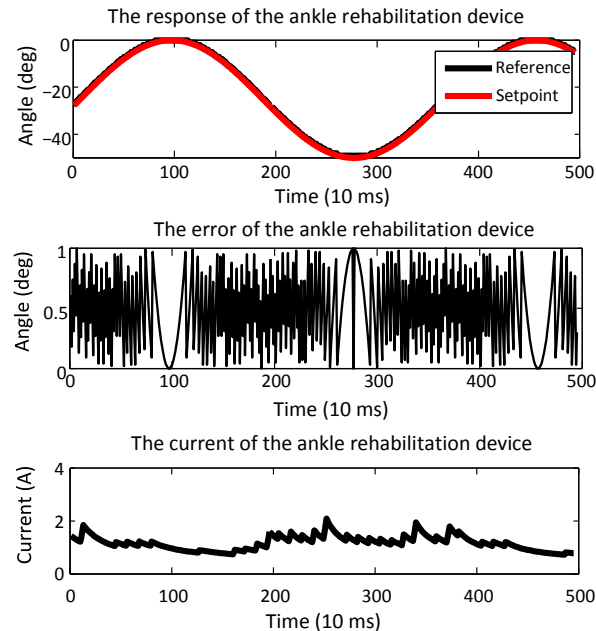


Fig. 12. Experiment results of plantarflexion exercise with humans. Graphs show setpoint angle (red) and measured angle (black) values for the device (top), angular error of the device (middle), current of the device (bottom)

5. Conclusion

In this paper, we have presented the kinematic model of the ankle rehabilitation device. We set up the dynamic equations and designed the sliding controller for the research model. The Matlab software simulated the device's response, and the results were obtained with fast response time and small rotational angle error. The simulation result for the maximum torque of the device is 8 Nm, which is equivalent to other research works [29, 30]. We also designed and manufactured a fully functional prototype of the ankle rehabilitation device, followed by clinical tests performed on volunteers. The results from our clinical trial indicate fast response time and small angular error. Test results on humans show that the device works safely and operates according to the installed trajectory.

Furthermore, the device has a simple design, operates smoothly, and is adaptable to different operating settings. Overall, we believe these are positive results, and our single DOF ankle rehabilitation device holds a lot of potential to help stroke patients. In the future, we will continue to refine the device's aesthetics and conduct patient trials to evaluate its effectiveness.

References

- [1] E. Osayande, K.P. Ayodele, M.A. Komolafe. Development of a robotic hand orthosis for stroke patient rehabilitation. *International Journal of Online and Biomedical Engineering*, 16(13):142–149, 2020. doi: [10.3991/ijoe.v16i13.13407](https://doi.org/10.3991/ijoe.v16i13.13407).
- [2] Z. Yue, X. Zhang, and J. Wang. Hand Rehabilitation robotics on poststroke motor recovery. *Behavioural Neurology*, 2017:3908135, 2017. doi: [10.1155/2017/3908135](https://doi.org/10.1155/2017/3908135).
- [3] C. Grefkes and G.R. Fink. Recovery from stroke: current concepts and futures perspectives. *Neurological Research and Practice*, 2(1):17, 2020. doi: [10.1186/s42466-020-00060-6](https://doi.org/10.1186/s42466-020-00060-6).
- [4] R. Gassert and V. Dietz. Rehabilitation robots for the treatment of sensorimotor deficits: a neurophysiological perspective. *Journal of NeuroEngineering and Rehabilitation*, 15:46, 2018. doi: [10.1186/s12984-018-0383-x](https://doi.org/10.1186/s12984-018-0383-x).
- [5] S.H. Hayes and S.R. Carroll. Early intervention care in the acute stroke patient. *Archives of Physical Medicine and Rehabilitation*, 67(5):319–321, 1986.
- [6] D.U. Jette, R.L. Warren, and C. Wirtalla. The relation between therapy intensity and outcomes of rehabilitation in skilled nursing facilities. *Archives of Physical Medicine and Rehabilitation*, 86(3):373–379, 2005. doi: [10.1016/j.apmr.2004.10.018](https://doi.org/10.1016/j.apmr.2004.10.018).
- [7] Z. Zhou and Q. Wang. Concept and prototype design of a robotic ankle-foot rehabilitation system with passive mechanism for coupling motion. *2019 IEEE 9th Annual International Conference on CYBER Technology in Automation, Control, and Intelligent Systems (CYBER)*, pages 1002–1005, Suzhou, China, 29 July -2 August, 2019. doi: [10.1109/cyber46603.2019.9066745](https://doi.org/10.1109/cyber46603.2019.9066745).
- [8] C.M. Racu and I. Doroftei. An overview on ankle rehabilitation devices. *Advanced Materials Research*, 1036:781–786, 2014. doi: [10.4028/www.scientific.net/amr.1036.781](https://doi.org/10.4028/www.scientific.net/amr.1036.781).
- [9] A.A. Blank, J.A. French, A.U. Pehlivan, and M.K. O'Malley. Rehabilitation: Current trends in robot-assisted upper-limb stroke rehabilitation: promoting patient engagement in therapy. *Current Physical Medicine and Rehabilitation Reports*, 2(3):184–195, 2014.

- [10] Z. Liao, L. Yao, Z. Lu, and J. Zhang. Screw theory based mathematical modeling and kinematic analysis of a novel ankle rehabilitation robot with a constrained 3-PSP mechanism topology. *International Journal of Intelligent Robotics and Applications*, 2(3):351–360, 2018. doi: [10.1007/s41315-018-0063-9](https://doi.org/10.1007/s41315-018-0063-9).
- [11] C.C.K. Lin, M.S. Ju, S.M. Chen, and B.W. Pan. A specialized robot for ankle rehabilitation and evaluation. *Journal of Medical and Biological Engineering*, 28(2):79–86, 2008.
- [12] Z. Sun et al. Mechanism Design and ADAMS-MATLAB-Simulation of a Novel Ankle Rehabilitation Robot. *2019 IEEE International Conference on Robotics and Biomimetic (ROBIO)*, pages 425–432, Dali, China, December, 2019. doi: [10.1109/robio49542.2019.8961829](https://doi.org/10.1109/robio49542.2019.8961829).
- [13] Q. Liu, A. Liu, W. Meng, Q. Ai, and S.Q. Xie. Hierarchical compliance control of a soft ankle rehabilitation robot actuated by pneumatic muscles. *Frontiers in Neurorobotics*, 11:64, 2017. doi: [10.3389/fnbot.2017.00064](https://doi.org/10.3389/fnbot.2017.00064).
- [14] T. Yonezawa, K. Nomura, T. Onodera, S. Ishimura, H. Mizoguchi, and H. Takemura. Evaluation of venous return in lower limb by passive ankle exercise performed by PHARAD. *2015 37th Annual International Conference of the IEEE Engineering in Medicine and Biology Society (EMBC)*, pages 3582–3585, Milan, Italia, 25–29 August, 2015. doi: [10.1109/embc.2015.7319167](https://doi.org/10.1109/embc.2015.7319167).
- [15] Ye Ding, M. Sivak, B. Weinberg, C. Mavroidis, and M.K. Holden. NUVABAT: Northeastern university virtual ankle and balance trainer. *2010 IEEE Haptics Symposium*, pages 509–514, Waltham, Massachusetts, USA, 25–26 March, 2010. doi: [10.1109/haptic.2010.5444608](https://doi.org/10.1109/haptic.2010.5444608).
- [16] D. Ao, R. Song, and J. Gao. Movement performance of human–robot cooperation control based on emg-driven hill-type and proportional models for an ankle power-assist exoskeleton robot. *IEEE Transactions on Neural Systems and Rehabilitation Engineering*, 25(8):1125–1134, 2017. doi: [10.1109/tnsre.2016.2583464](https://doi.org/10.1109/tnsre.2016.2583464).
- [17] Y. Ren, Y.-N. Wu, C.-Y. Yang, T. Xu, R. L. Harvey, and L.-Q. Zhang. Developing a wearable ankle rehabilitation robotic device for in-bed acute stroke rehabilitation. *IEEE Transactions on Neural Systems and Rehabilitation Engineering*, 25(6):589–596, 2017. doi: [10.1109/tnsre.2016.2584003](https://doi.org/10.1109/tnsre.2016.2584003).
- [18] G. Aguirre-Ollinger, J.E. Colgate, M.A. Peshkin, and A. Goswami. Design of an active one-degree-of-freedom lower-limb exoskeleton with inertia compensation. *The International Journal of Robotics Research*, 30(4):486–499, 2011. doi: [10.1177/0278364910385730](https://doi.org/10.1177/0278364910385730).
- [19] Z. Zhou, Y. Sun, N. Wang, F. Gao, K. Wei, and Q. Wang. Robot-assisted rehabilitation of ankle plantar flexors spasticity: a 3-month study with proprioceptive neuromuscular facilitation. *Frontiers in Neurorobotics*, 10:16, 2016. doi: [10.3389/fnbot.2016.00016](https://doi.org/10.3389/fnbot.2016.00016).
- [20] I. Doroftei, C.M. Racu, C. Honceriu, and D. Irimia. One-degree-of-freedom ankle rehabilitation platform. *IOP Conference Series: Materials Science and Engineering*, 591:012076, 2019. doi: [10.1088/1757-899x/591/1/012076](https://doi.org/10.1088/1757-899x/591/1/012076).
- [21] A. Gmerek and E. Jezierski. Admittance control of a 1-DoF robotic arm actuated by BLDC motor. *2012 17th International Conference on Methods & Models in Automation & Robotics (MMAR)*, pages 633–638, Miedzyzdroje, Poland, 27–30 August, 2012. doi: [10.1109/m-mar.2012.6347811](https://doi.org/10.1109/m-mar.2012.6347811).
- [22] Ł. Woliński. Comparison of the adaptive and neural network control for LWR 4+ manipulators: simulation study. *Archive of Mechanical Engineering*, 67(1):111–121, 2020. doi: [10.24425/ame.2020.131686](https://doi.org/10.24425/ame.2020.131686).
- [23] Meera C S, M.K. Gupta, and S. Mohan. Disturbance observer-assisted hybrid control for autonomous manipulation in a robotic backhoe. *Archive of Mechanical Engineering*, 66(2):153–169, 2019. doi: [10.24425/ame.2019.128442](https://doi.org/10.24425/ame.2019.128442).
- [24] O. Jedda, J. Ghabi and A. Douik. Sliding mode control of an inverted pendulum. In: Derbel N., Ghommam J., Zhu Q. (eds), *Applications of Sliding Mode Control. Studies in Systems, Decision and Control*, chapter 6:105–118, 2016, Springer. doi: [10.1007/978-981-10-2374-3_6](https://doi.org/10.1007/978-981-10-2374-3_6).

- [25] S. Singh, M.S. Qureshi, and P. Swarnkar. Comparison of conventional PID controller with sliding mode controller for a 2-link robotic manipulator. *2016 International Conference on Electrical Power And Energy System (ICEPES)*, pages 115–119, Bhopal, India, 14-16 December, 2016. doi: [10.1109/icepes.2016.7915916](https://doi.org/10.1109/icepes.2016.7915916).
- [26] P. Boscaroli and D. Richiedei. Trajectory design for energy savings in redundant robotic cells. *Robotics*, 8(1):15, 2019. doi: [10.3390/robotics8010015](https://doi.org/10.3390/robotics8010015).
- [27] M. Adolphe, J. Clerval, Z. Kirchof, R. Lacombe-Delpech, and B. Zagrodny. Center of mass of human's body segments, *Mechanics and Mechanical Engineering*, 21(3):485–497, 2017.
- [28] T. Eiammanussakul and V. Sangveraphunsiri. A lower limb rehabilitation robot in sitting position with a review of training activities. *Journal of Healthcare Engineering*, 2018:927807, 2018. doi: [10.1155/2018/1927807](https://doi.org/10.1155/2018/1927807).
- [29] A. Roy, H.I. Krebs, C.T. Bever, L.W. Forrester, R.F. Macko, and N. Hogan. Measurement of passive ankle stiffness in subjects with chronic hemiparesis using a novel ankle robot. *Journal of Neurophysiology*, 105(5):2132–2149, 2011. doi: [10.1152/jn.01014.2010](https://doi.org/10.1152/jn.01014.2010).
- [30] F. Gao, Y. Ren, E.J. Roth, R. Harvey, and L.-Q. Zhang. Effects of repeated ankle stretching on calf muscle–tendon and ankle biomechanical properties in stroke survivors. *Clinical Biomechanics*, 26(5):516–522, 2011. doi: [10.1016/j.clinbiomech.2010.12.003](https://doi.org/10.1016/j.clinbiomech.2010.12.003).
- [31] G. Bucca, A. Bezzolato, S. Bruni and F. Molteni. A Mechatronic Device for the Rehabilitation of Ankle Motor Function. *Journal of Biomechanical Engineering*, 131(12):125001, 2009. doi: [10.1115/1.4000083](https://doi.org/10.1115/1.4000083).
- [32] J. Zhong, Y. Zhu, C. Zhao, Z. Han, and X. Zhang. Position tracking of a pneumatic-muscle-driven rehabilitation robot by a single neuron tuned pid controller. *Complexity*, 2020:438391, 2020. doi: [10.1155/2020/1438391](https://doi.org/10.1155/2020/1438391).